

Gauge-invariant field-strength correlators in pure Yang-Mills and full QCD at finite temperature *

M. D'Elia

Dipartimento di Fisica,
Università di Genova,
and INFN, Sezione di Genova,
I-16146 Genova, Italy.

A. Di Giacomo, E. Meggiolaro

Dipartimento di Fisica,
Università di Pisa,
and INFN, Sezione di Pisa,
I-56127 Pisa, Italy.

Abstract

We study by numerical simulations on a lattice the behaviour of the gauge-invariant two-point correlation functions of the gauge-field strengths across the deconfinement phase transition, both for the pure-gauge $SU(3)$ theory and for full QCD with two flavours. *Quenched* data agree within errors with previous determinations, but have much higher statistics. A best-fit analysis of the data has been performed, both for the *quenched* and the full-QCD case, showing that the electric gluon condensate drops to zero at the deconfining phase transition.

(PACS codes: 12.38.Gc, 11.10.Wx)

*Partially supported by MIUR (Italian Ministry of the University and of Scientific and Technological Research) and by the INTAS contract 00-0110.

1. Introduction

Gauge-invariant correlation functions of the field strengths in the QCD vacuum play an important role in high-energy phenomenology and in stochastic models of QCD, both at zero temperature [1, 2, 3] and non-zero temperature [4, 5, 6]. For a recent review see Ref. [7]. Some years ago, a determination of such correlators at finite temperature was done on a $16^3 \times 4$ lattice, for the pure-gauge $SU(3)$ theory, in a range of distances from 0.4 to 1 fm approximately [8, 9]. The technique used to make the computation feasible is a local cooling of the configurations: this procedure freezes local fluctuations, leaving long-range correlations unchanged. In this paper, prompted by the progresses of the stochastic-vacuum approach to QCD [10], we improve the determination of the correlators at finite temperature $T \sim T_c$ for pure gauge $SU(3)$, by use of a larger lattice ($32^3 \times 6$) and bigger statistics. We also compute the correlators at $T = 0$ and at $T \sim T_c$ in full QCD with 2 staggered dynamical quarks. In Sect. 2 we recall the notation. The numerical results are presented in Sect. 3, while Sect. 4 contains an analysis of the data and a discussion.

2. Notation

To simulate the system at finite temperature, a lattice is used of spatial extent $N_\sigma \gg N_\tau$, N_τ being the temporal extent, with periodic boundary conditions for gluons, and antiperiodic boundary conditions for fermions in the temporal direction. The temperature T corresponding to a given value of $\beta = 6/g^2$ is given by

$$N_\tau \cdot a = \frac{1}{T} , \tag{2.1}$$

where a is the lattice spacing. In the *quenched* case a only depends on the coupling β and, from renormalization group arguments,

$$a(\beta) = \frac{1}{\Lambda_L} f(\beta) , \tag{2.2}$$

where $f(\beta)$ is the so-called *scaling function* and Λ_L is the scale parameter of QCD in the lattice regularization scheme. At large enough β , $f(\beta)$ is given by the usual two-loop expression:

$$f(\beta) = \left(\frac{8}{33}\pi^2\beta\right)^{51/121} \exp\left(-\frac{4}{33}\pi^2\beta\right) [1 + \mathcal{O}(1/\beta)] , \quad (2.3)$$

for gauge group $SU(3)$ and in the absence of quarks. The expression (2.3) can also be used in a small enough interval of β 's lower than the asymptotic scaling region, and then Λ_L is an effective scale depending on the position of the interval considered. For the range of values of β 's that we have considered (see below), its value, extracted from the string tension [11, 12], is about 4.9 MeV.

The gauge-invariant two-point correlators of the field strengths in the QCD vacuum are defined as [1, 2, 3]

$$\mathcal{D}_{\mu\rho,\nu\sigma}(x) = g^2 \langle \text{Tr}[G_{\mu\rho}(0)S(0,x)G_{\nu\sigma}(x)S^\dagger(0,x)] \rangle , \quad (2.4)$$

where $G_{\mu\rho} = T^a G_{\mu\rho}^a$ is the field-strength tensor, T^a are the generators of the algebra of the gauge group in the fundamental representation, and

$$S(0,x) = \text{P exp} \left(ig \int_0^1 dt x^\mu A_\mu(xt) \right) \quad (2.5)$$

is the Schwinger parallel transport from 0 to x along a straight-line path;* $A_\mu \equiv T^a A_\mu^a$. At zero temperature, that is on a symmetric lattice $N_\sigma = N_\tau$, the correlators are expressed in terms of two independent invariant functions of x^2 , known as $\mathcal{D}(x^2)$ and $\mathcal{D}_1(x^2)$ [1, 2, 3]:

$$\begin{aligned} \mathcal{D}_{\mu\rho,\nu\sigma}(x) = & (\delta_{\mu\nu}\delta_{\rho\sigma} - \delta_{\mu\sigma}\delta_{\rho\nu}) [\mathcal{D}(x^2) + \mathcal{D}_1(x^2)] \\ & + (x_\mu x_\nu \delta_{\rho\sigma} - x_\mu x_\sigma \delta_{\rho\nu} + x_\rho x_\sigma \delta_{\mu\nu} - x_\rho x_\nu \delta_{\mu\sigma}) \frac{\partial \mathcal{D}_1(x^2)}{\partial x^2} . \end{aligned} \quad (2.6)$$

At finite temperature ($N_\sigma \gg N_\tau$) the $O(4)$ space-time symmetry is broken down to the spatial $O(3)$ symmetry and the bilocal correlators are now expressed in terms of five independent functions [4, 5, 6]. Two of them are needed to describe the electric-electric

*Recently a strong dependence of the correlators on the shape of the path in the Schwinger string has been found numerically [13]. However, the stochastic-vacuum models naturally select the straight-line path. For that reason, we limit our present analysis to the straight-line Schwinger string.

correlations:

$$\begin{aligned}
& g^2 \langle \text{Tr}[E_i(x)S(x, y)E_k(y)S^\dagger(x, y)] \rangle \\
& = \delta_{ik} \left[D^E + D_1^E + u_4^2 \frac{\partial D_1^E}{\partial u_4^2} \right] + u_i u_k \frac{\partial D_1^E}{\partial \vec{u}^2},
\end{aligned} \tag{2.7}$$

where $E_i = G_{i4}$ is the electric field operator and $u_\mu = x_\mu - y_\mu$ [$\vec{u}^2 = (\vec{x} - \vec{y})^2$].

Two further functions are needed for the magnetic–magnetic correlations:

$$\begin{aligned}
& g^2 \langle \text{Tr}[B_i(x)S(x, y)B_k(y)S^\dagger(x, y)] \rangle \\
& = \delta_{ik} \left[D^B + D_1^B + \vec{u}^2 \frac{\partial D_1^B}{\partial \vec{u}^2} \right] - u_i u_k \frac{\partial D_1^B}{\partial \vec{u}^2},
\end{aligned} \tag{2.8}$$

where $B_k = \frac{1}{2}\varepsilon_{ijk}G_{ij}$ is the magnetic field operator.

Finally, one more function is necessary to describe the mixed electric–magnetic correlations:

$$g^2 \langle \text{Tr}[E_i(x)S(x, y)B_k(y)S^\dagger(x, y)] \rangle = -\frac{1}{2}\varepsilon_{ikn}u_n \frac{\partial D_1^{BE}}{\partial u_4}. \tag{2.9}$$

In Eqs. (2.7), (2.8) and (2.9), the five quantities D^E , D_1^E , D^B , D_1^B and D_1^{BE} are all functions of \vec{u}^2 , due to rotational invariance, and of u_4^2 , due to time–reversal invariance.

From the conclusions of Refs. [4, 5, 6], one expects that D^E is related to the (temporal) string tension and should have a drop just above the deconfinement critical temperature T_c . In other words, D^E is expected to be a kind of order parameter for confinement; on the contrary, D_1^E does not contribute to the area law of the temporal Wilson loop. Similarly, D^B is related to the spatial string tension [4, 5], while D_1^B does not contribute to the area law of the spatial Wilson loop.

The above arguments hold both for the *quenched* and the *unquenched* theory, with a suitable modification of Eq. (2.2) and (2.3). In particular for the full–QCD case, in order to fix the scale, we have used the lattice spacing as determined in [14].

3. Results

We have determined the following four quantities [15]

$$\begin{aligned}\mathcal{D}_{\parallel}^E(\vec{u}^2, 0) &\equiv \mathcal{D}^E(\vec{u}^2, 0) + \mathcal{D}_1^E(\vec{u}^2, 0) + \vec{u}^2 \frac{\partial \mathcal{D}_1^E}{\partial \vec{u}^2}(\vec{u}^2, 0) ; \\ \mathcal{D}_{\perp}^E(\vec{u}^2, 0) &\equiv \mathcal{D}^E(\vec{u}^2, 0) + \mathcal{D}_1^E(\vec{u}^2, 0) ;\end{aligned}\tag{3.1}$$

$$\begin{aligned}\mathcal{D}_{\parallel}^B(\vec{u}^2, 0) &\equiv \mathcal{D}^B(\vec{u}^2, 0) + \mathcal{D}_1^B(\vec{u}^2, 0) + \vec{u}^2 \frac{\partial \mathcal{D}_1^B}{\partial \vec{u}^2}(\vec{u}^2, 0) ; \\ \mathcal{D}_{\perp}^B(\vec{u}^2, 0) &\equiv \mathcal{D}^B(\vec{u}^2, 0) + \mathcal{D}_1^B(\vec{u}^2, 0) ,\end{aligned}\tag{3.2}$$

by measuring appropriate linear superpositions of the correlators (2.7) and (2.8) at equal times ($u_4 = 0$). Concerning the mixed electric–magnetic correlator of Eq. (2.9), it vanishes both at zero temperature and at finite temperature, when computed at equal times ($u_4 = 0$), as a consequence of the invariance of the theory under time reversal.

We have chosen a $32^3 \times 6$ lattice (so that, in our notation, $N_\tau = 6$) for the *quenched* case. The critical temperature T_c for such a lattice corresponds to $\beta_c \simeq 5.89$ [16]. For full QCD we have used 2 species of staggered fermions with bare mass $a \cdot m = 0.0125$ and a $32^3 \times 8$ lattice, for which T_c corresponds to a coupling $\beta_c \simeq 5.54$ [17]. The standard “R–version” of the HMC algorithm [18] has been used in the full–QCD case.

For the *quenched* theory the behaviour of $\mathcal{D}_{\parallel}^E$ and \mathcal{D}_{\perp}^E is shown in Figs. 1 and 2 respectively, at different values of T/T_c with the physical distance in the range from ~ 0.25 fm up to ~ 1.25 fm. A clear drop is observed for $\mathcal{D}_{\parallel}^E$ and \mathcal{D}_{\perp}^E across the phase transition, as expected. The analogous behaviour for $\mathcal{D}_{\parallel}^B$ and \mathcal{D}_{\perp}^B is shown in Figs. 3 and 4. No dramatic change is visible across the transition for the magnetic correlations. These behaviours of the correlators were already known from Refs. [8, 9], with which we agree within the errors. In Figs. 1–4 the thick continuum line has been obtained using the parameters of the best fit at $T = 0$ obtained in Ref. [8], Eqs. (2.10) and (2.11).

In Figs. 5–8 we present the analogous data for the case with dynamical fermions. In full QCD previous results at $T = 0$ have been reported only for the case of 4 flavours [19]. Therefore, in order to compare with $T = 0$, we have performed a simulation at $\beta = 5.55$ on a 16^4 lattice: the results are reported in the same figures. Also in this case it is apparent that $\mathcal{D}_{\parallel}^E$ and \mathcal{D}_{\perp}^E stay almost constant at their zero–temperature value up to the phase transition, where they undergo a sharp drop. Instead no dramatic change is visible for the magnetic correlators.

Our results, both for the *quenched* and the full-QCD case, are in agreement with those already found in Refs. [8, 9] and can be summarized as follows:

- (1) In the confined phase ($T < T_c$), up to temperatures very near to T_c , the correlators, both the electric–electric type (2.7) and the magnetic–magnetic type (2.8), are nearly equal to the correlators at zero temperature: in other words, $D^E \simeq D^B \simeq D$ and $D_1^E \simeq D_1^B \simeq D_1$ for $T < T_c$.
- (2) Immediately above T_c , the electric–electric correlators (2.7) have a clear drop, while the magnetic–magnetic correlators (2.8) stay almost unchanged, or show a slight increase.

In the next section we shall report on a quantitative analysis of the data displayed in Figs. 1–8.

4. Quantitative analysis

Inspired by our previous analyses of the correlators in the $T = 0$ case (see Refs. [15, 8, 19] and also [20]), we have performed best fits to the lattice data for the correlators (3.1) and (3.2) at finite temperature T (and at equal times, i.e., $u_4 = 0$), with the functions (here $x = |\vec{u}|$):

$$\mathcal{D}^E(x) = A_0 e^{-\mu_A x} + \frac{a_0}{x^4} \quad , \quad \mathcal{D}_1^E(x) = A_1 e^{-\mu_A x} + \frac{a_1}{x^4} \quad , \quad (4.1)$$

$$\mathcal{D}^B(x) = B_0 e^{-\mu_B x} + \frac{b_0}{x^4} \quad , \quad \mathcal{D}_1^B(x) = B_1 e^{-\mu_B x} + \frac{b_1}{x^4} \quad , \quad (4.2)$$

where, of course, all the coefficients must be considered as functions of the physical temperature T . The four independent functions (4.1) and (4.2) are written as the sum of a *non-perturbative* exponential term plus a *perturbative-like* term behaving as $1/x^4$ (in fact, a term of this form is predicted by ordinary perturbation theory).^{*} In Refs. [8, 19] the perturbative-like term had the form $\sim e^{-\mu_a x}/x^4$: the exponential term $e^{-\mu_a x}$ has been

^{*}Of course the coefficient of $1/x^4$ is regularization–scheme dependent. In Eqs. (4.1) and (4.2) we refer to the lattice regularization scheme; other schemes could give different values [21].

neglected here (i.e., we fix $\mu_a = 0$), since, in the spirit of the Operator Product Expansion (OPE), we will concentrate on the behaviour of the correlators at short distances.

Two quantities of physical interest enter in our best fits to the lattice data:

- (1) The correlation length of the gluon field strengths, defined as $\lambda_A = 1/\mu_A$ for the electric correlators and $\lambda_B = 1/\mu_B$ for the magnetic correlators. (*A priori*, we distinguish the two correlation lengths λ_A and λ_B in the parametrization (4.1)–(4.2). However, as we shall see below, we have found that our data can be well fitted using the same correlation length $\lambda_A = \lambda_B$ for the electric and the magnetic correlators.)
- (2) The gluon condensate, defined as

$$G_2 \equiv \left\langle \frac{\alpha_s}{\pi} : G_{\mu\nu}^a G_{\mu\nu}^a : \right\rangle \quad (\alpha_s = \frac{g^2}{4\pi}) . \quad (4.3)$$

These two quantities play an important role in phenomenology. The correlation length is relevant for the description of vacuum models [1, 2, 3].

The gluon condensate was first introduced in Ref. [22], in the context of the SVZ sum rules. As pointed out in Refs. [19, 20], lattice provides us with a regularized determination of the correlators. We shall briefly repeat here the argumentation originally reported in Refs. [19, 20]. As in Ref. [22], our correlators can be given an OPE [23]:

$$\frac{1}{2\pi^2} \mathcal{D}_{\mu\nu,\mu\nu}(x) \underset{x \rightarrow 0}{\sim} C_1(x) \langle \mathbf{1} \rangle + C_g(x) G_2 + \sum_{f=1}^{N_f} C_f(x) m_f \langle : \bar{q}_f q_f : \rangle + \dots , \quad (4.4)$$

if we have N_f quark flavours with masses m_f . (Of course, the last term in Eq. (4.4), i.e., the mixing to the quark condensates, is absent in the *quenched* theory.) The mixing to the identity operator $C_1(x)$ has a $1/x^4$ behaviour at small x . The mixings to the operators of dimension four $C_g(x)$ and $C_f(x)$ are expected to behave as constants for $x \rightarrow 0$. Higher-order terms in the OPE (4.4) are neglected. The coefficients of the Wilson expansion are usually determined in perturbation theory and are known to be plagued by the so-called “infrared renormalons” (see for example Ref. [24] and references therein). In the same spirit of Ref. [22], we shall disregard the renormalon ambiguity, as we did in Ref. [19]. With the normalization of Eq. (4.4), this gives $C_g(0) \simeq 1$. The contribution from the

quark operators in (4.4) can be neglected because it is higher order in $1/\beta$. The gluon condensate is then, using the parametrization (4.1)–(4.2) for the correlators:

$$G_2 = \frac{3}{\pi^2}(A_0 + A_1 + B_0 + B_1) . \quad (4.5)$$

G_2 is the sum of an *electric* contribution, that we shall call $G_2^{(ele)}$, plus a *magnetic* contribution, that we shall call $G_2^{(mag)}$, which at non-zero temperature T are in general different and should be distinguished:

$$G_2^{(ele)} \equiv \frac{g^2}{\pi^2} \langle : \text{Tr}[\vec{E}^2] : \rangle ; \quad G_2^{(mag)} \equiv \frac{g^2}{\pi^2} \langle : \text{Tr}[\vec{B}^2] : \rangle . \quad (4.6)$$

When using the parametrization (4.1)–(4.2) for the correlators, one easily finds that:

$$G_2^{(ele)} = \frac{3}{\pi^2}(A_0 + A_1) ; \quad G_2^{(mag)} = \frac{3}{\pi^2}(B_0 + B_1) . \quad (4.7)$$

Let us discuss now the results obtained from the best fits to our data with the functions (4.1)–(4.2). First of all, we have tried a best fit to the data for the magnetic correlators (3.2) with the functions (4.2), where the mass μ_B of the non-perturbative exponential terms has been put equal to the corresponding value obtained in the $T = 0$ case:

$$\begin{aligned} \mu_B &= 4.53(7) \text{ fm}^{-1} \quad (\textit{quenched}) ; \\ \mu_B &= 3.5(2) \text{ fm}^{-1} \quad (\text{full QCD}) . \end{aligned} \quad (4.8)$$

The *quenched* value has been taken from Ref. [8], Eqs. (2.10) and (2.11); the correlators at $T = 0$ are reproduced by the thick lines in Figs. 1–4. Instead, the full-QCD value has been extracted from a best fit to the new data at $T = 0$ ($\beta = 5.55$ on a 16^4 lattice), reported in Figs. 5–8. The magnetic correlators are well fitted, up to distances of about $x \simeq 0.8$ fm, by the functions (4.2) with the mass μ_B fixed to the value given in Eq. (4.8).

The results obtained for all the various cases are reported in Table I. From these results one sees that all the coefficients, B_0 , B_1 , b_0 and b_1 , are rather stable, when varying the temperature T : only the non-perturbative coefficient B_0 shows a slight increase when increasing T , so that, by virtue of Eq. (4.7), we can say that the magnetic gluon condensate $G_2^{(mag)}$ slightly increases across the transition at T_c [see Fig. 9]. Let us also

observe that the pure-gauge magnetic gluon condensate is sensibly higher than the corresponding value in the full-QCD case: this is in agreement with the fact that the gluon condensate G_2 is expected to increase with the quark mass [25], tending towards the asymptotic (pure-gauge) value, as already checked on data at $T = 0$ [19]. The stability of the perturbative coefficients b_0 and b_1 is expected since they are UV-dominated cut-off terms. More precisely, these perturbative coefficients are practically independent on the lattice volume ($N_\sigma^3 \times N_\tau$), as one can verify by direct computation [26]. In general, (at a fixed lattice volume $N_\sigma^3 \times N_\tau$) they depend on β and it is known that $b_0 = \mathcal{O}(1/\beta^2)$ and $b_1 = \mathcal{O}(1/\beta)$. However, in the range of values of T that we have considered, $\Delta\beta/\beta \ll 1$ and the β dependence of the perturbative coefficients can be neglected within the errors. For the same reasons, these magnetic perturbative coefficients should be practically equal to the corresponding coefficients a_0 and a_1 in the electric correlators (4.1).

Therefore, on the basis of these considerations, we have tried a best fit to the data for the electric correlators (3.1) for distances from 3 up to 5–6 lattice spacings (corresponding approximately to the range of physical distances $0.3 \div 0.6$ fm),[†] with the functions (4.1), where the perturbative coefficients a_0 and a_1 have been fixed to the (weighted) average values of the corresponding magnetic coefficients b_0 and b_1 reported in Table I for all the temperatures that we have considered:

$$\begin{aligned} a_0 &= 0.55(2) \quad ; \quad a_1 = 0.35(1) \quad (\text{quenched}) \quad ; \\ a_0 &= 0.64(2) \quad ; \quad a_1 = 0.33(1) \quad (\text{full QCD}) \quad . \end{aligned} \tag{4.9}$$

Moreover, we have fixed the mass μ_A of the non-perturbative exponential terms in (4.1) to the same value μ_B used for the magnetic correlators [Eq. (4.8)], which is in turn the value at $T = 0$. In Table II we report the results obtained for the perpendicular electric correlator \mathcal{D}_\perp^E [see Eq. (3.1)]. The coefficient $A_0 + A_1$ of the non-perturbative part of the correlator, which, by virtue of Eq. (4.7), is proportional to the electric gluon condensate $G_2^{(ele)}$, sharply decreases across the transition [see Fig. 10]. Again, we find that the pure-gauge electric gluon condensate is sensibly higher than the corresponding value in the full-QCD case, in agreement with the general claim done in Ref. [25].

Finally, we have performed a best fit to the values for the difference

$$\mathcal{D}_\perp^E(x) - \mathcal{D}_\parallel^E(x) = -\frac{x}{2} \frac{\partial \mathcal{D}_1^E}{\partial x}(x) \tag{4.10}$$

[†]This is the range of distances where we have data for the parallel electric correlator at all temperatures.

between the two quantities displayed in Figs. 2 and 1 respectively (Figs. 6 and 5 for the full-QCD case). The results are reported in Table III. Since (from previous experience at $T = 0$) the quantity in the r.h.s. of Eq. (4.10) is expected to be dominated by the perturbative term, in this case we have left also the coefficient a_1 as a free parameter in the fit, in order to test the validity of the assumption that the perturbative coefficients are temperature independent. The test is perfect for the *quenched* case and reasonable for the full-QCD case. One finds that the coefficient A_1 of the non-perturbative part of the function \mathcal{D}_1^E stays compatible with zero, within the (large) errors, across the phase transition at T_c . So the clear drop seen in the quantities \mathcal{D}_\parallel^E and \mathcal{D}_\perp^E across T_c seems to be entirely due to the coefficient A_0 of the non-perturbative part of the function \mathcal{D}^E alone. This result is consistent with Refs. [8, 9] and again confirms the conclusion of Refs. [4, 5, 6], where \mathcal{D}^E (or, better, its non-perturbative part) was related to the (*temporal*) string tension σ_E . It was also shown in Refs. [4, 5] that \mathcal{D}^B (or, better, its non-perturbative part) is related to the *spatial* string tension σ_s . Existing lattice results [27, 28, 16] indicate that σ_s is almost constant around T_c and increases for $T \geq 2T_c$: this fact is in good agreement with the behaviour that we find for the coefficient B_0 of the non-perturbative part of the function \mathcal{D}^B (see Table I).

In summary, our best-fit analysis of the data leads to the following conclusions:

- (1) The correlation lengths $\lambda_A = 1/\mu_A$ for the electric correlators [Eq. (4.1)] and $\lambda_B = 1/\mu_B$ for the magnetic correlators [Eq. (4.2)] are equal and do not change across the deconfining phase transition at T_c .
- (2) The electric gluon condensate, defined in Eqs. (4.6) and (4.7), drops to zero at $T = T_c$, whilst the magnetic gluon condensate is practically unchanged, showing a small increase [see Figs. 9 and 10].
- (3) As expected, the coefficients of the perturbative terms are temperature independent and are the same for the magnetic and the electric correlators.

Acknowledgements

Part of this work was done using the CRAY T3E of the CINECA Inter University Computing Centre (Bologna, Italy). We would like to thank the CINECA for the kind and highly qualified technical assistance.

Stimulating discussions with Yuri Simonov are warmly acknowledged.

References

- [1] H.G. Dosch, Phys. Lett. B **190** (1987) 177.
- [2] H.G. Dosch and Yu.A. Simonov, Phys. Lett. B **205** (1988) 339.
- [3] Yu.A. Simonov, Nucl. Phys. B **324** (1989) 67.
- [4] Yu.A. Simonov, JETP Lett. **54** (1991) 249.
- [5] Yu.A. Simonov, JETP Lett. **55** (1992) 627; Yad. Fiz. **58** (1995) 357.
- [6] Yu.A. Simonov and E.L. Gubankova, Phys. Lett. B **360** (1995) 93.
- [7] A. Di Giacomo, H.G. Dosch, V.I. Shevchenko and Yu.A. Simonov, Phys. Rep. C **372** (2002) 319.
- [8] A. Di Giacomo, E. Meggiolaro and H. Panagopoulos, Nucl. Phys. B **483** (1997) 371.
- [9] A. Di Giacomo, E. Meggiolaro and H. Panagopoulos, Pisa preprint IFUP–TH 14/96 (1996); Cyprus preprint UCY–PHY–96/6 (1996); hep-lat/9603018.
- [10] D.S. Kuzmenko and Yu.A. Simonov, Phys. Atom. Nucl. **64** (2001) 1887; Yad. Fiz. **64** (2001) 1971.
- [11] C. Michael and M. Teper, Phys. Lett. B **206** (1988) 299.
- [12] G.S. Bali and K. Schilling, Phys. Rev. D **47** (1993) 661.
- [13] A. Di Giacomo and E. Meggiolaro, Phys. Lett. B **537** (2002) 173.
- [14] B. Alles, M. D’Elia and A. Di Giacomo, Phys. Lett. B **483** (2000) 189.
- [15] A. Di Giacomo and H. Panagopoulos, Phys. Lett. B **285** (1992) 133.
- [16] G. Boyd, J. Engels, F. Karsch, E. Laermann, C. Legeland, M. Lütgemeier and B. Petersson, Nucl. Phys. B **469** (1996) 419.
- [17] S. Gottlieb, A. Krasnitz, U.M. Heller, A.D. Kennedy, J.B. Kogut, R.L. Renken, D.K. Sinclair, R.L. Sugar, D. Toussaint and K.C. Wang, Phys. Rev. D **47** (1993) 3619.

- [18] S. Gottlieb, W. Liu, D. Toussaint, R.L. Renken and R.L. Sugar, Phys. Rev. D **35** (1987) 2531.
- [19] M. D’Elia, A. Di Giacomo and E. Meggiolaro, Phys. Lett. B **408** (1997) 315.
- [20] E. Meggiolaro, Phys. Lett. B **451** (1999) 414.
- [21] M. Eidemüller and M. Jamin, Phys. Lett. B **416** (1998) 415.
- [22] M.A. Shifman, A.I. Vainshtein, and V.I. Zakharov, Nucl. Phys. B **147** (1979) 385; 448; 519.
- [23] K.G. Wilson, Phys. Rev. **179** (1969) 1499.
- [24] A.H. Mueller, Nucl. Phys. B **250** (1985) 327;
A.H. Mueller, in *QCD, 20 Years Later*, edited by P.M. Zerwas and H.A. Kastrup (World Scientific, Singapore, 1993).
- [25] V.A. Novikov, M.A. Shifman, A.I. Vainshtein, and V.I. Zakharov, Nucl. Phys. B **191** (1981) 301.
- [26] M. Campostrini, A. Di Giacomo and G. Mussardo, Z. Phys. C **25** (1984) 173.
- [27] G.S. Bali, J. Fingberg, U.M. Heller, F. Karsch and K. Schilling, Phys. Rev. Lett. **71** (1993) 3059.
- [28] E. Laermann, Nucl. Phys. B (Proc. Suppl.) **42** (1995) 120.

TABLE CAPTIONS

Tab. I. Results obtained from a best fit to the data of the magnetic correlators (3.2) with the functions (4.2), for the various temperatures that we have examined: “q” stands for “*quenched*” data, while “f” stands for “full-QCD” data. The mass μ_B of the non-perturbative exponential terms has been put equal to the corresponding value obtained in the $T = 0$ case [Eq. (4.8)]. An asterisk (*) near the value of some parameter means that the parameter was an input for the best-fit.

Tab. II. Results obtained from a best fit to the data of the perpendicular electric correlator \mathcal{D}_\perp^E [see Eq. (3.1)] with the functions (4.1), where the perturbative coefficients a_0 and a_1 have been fixed to the (weighted) average values of the corresponding magnetic coefficients b_0 and b_1 reported in Table I for all the temperatures that we have considered [see Eq. (4.9)]. Moreover, we have fixed the mass μ_A of the non-perturbative exponential terms in (4.1) to the same value μ_B used for the magnetic correlators [Eq. (4.8)], i.e., to the corresponding value obtained in the $T = 0$ case. The notation used is the same as in Table I.

Tab. III. Results obtained from a best fit to the data of the difference between the perpendicular electric correlator \mathcal{D}_\perp^E and the parallel electric correlator \mathcal{D}_\parallel^E [see Eqs. (4.10) and (3.1)] with the functions (4.1), where the mass μ_A of the non-perturbative exponential terms in (4.1) has been fixed to the same value used in Table II. The notation used is the same as in Tables I and II.

Table I

theory	T/T_c	B_0 (10^8 MeV^4)	B_1 (10^8 MeV^4)	μ_B (fm^{-1})	b_0	b_1	χ^2/N
q	0.952	1320(70)	62(70)	4.53 (*)	0.54(5)	0.28(3)	0.7
q	0.974	1290(73)	-50(70)	4.53 (*)	0.60(5)	0.36(3)	1.2
q	1.007	1240(52)	-51(54)	4.53 (*)	0.57(4)	0.36(3)	0.6
q	1.030	1436(63)	24(77)	4.53 (*)	0.51(5)	0.34(3)	0.5
q	1.065	1305(54)	-55(70)	4.53 (*)	0.56(4)	0.37(3)	1.1
q	1.127	1455(49)	91(67)	4.53 (*)	0.50(4)	0.35(3)	1.9
q	1.261	1490(38)	17(60)	4.53 (*)	0.54(3)	0.36(2)	0.5
f	0.73	446(25)	37(16)	3.5 (*)	0.59(5)	0.19(4)	1.7
f	0.94	461(23)	24(24)	3.5 (*)	0.66(5)	0.30(3)	1.4
f	1.02	463(18)	-22(21)	3.5 (*)	0.63(4)	0.37(2)	0.63
f	1.18	510(30)	-11(27)	3.5 (*)	0.64(3)	0.40(3)	0.23
f	1.48	574(35)	8(34)	3.5 (*)	0.65(3)	0.38(2)	1.6

Table II

theory	T/T_c	$A_0 + A_1$ (10^8 MeV^4)	μ_A (fm^{-1})	$a_0 + a_1$	χ^2/N
q	0.952	1193(30)	4.53 (*)	0.90 (*)	0.2
q	0.974	930(25)	4.53 (*)	0.90 (*)	1.6
q	1.007	596(31)	4.53 (*)	0.90 (*)	2.1
q	1.030	318(42)	4.53 (*)	0.90 (*)	0.9
q	1.065	197(27)	4.53 (*)	0.90 (*)	0.2
q	1.127	56(60)	4.53 (*)	0.90 (*)	0.3
q	1.261	-88(57)	4.53 (*)	0.90 (*)	0.4
f	0.73	381(10)	3.5 (*)	0.97 (*)	0.2
f	0.94	413(20)	3.5 (*)	0.97 (*)	0.84
f	1.02	288(25)	3.5 (*)	0.97 (*)	1.9
f	1.18	186(30)	3.5 (*)	0.97 (*)	3.4
f	1.48	43(25)	3.5 (*)	0.97 (*)	3.3

Table III

theory	T/T_c	A_1 (10^8 MeV^4)	μ_A (fm^{-1})	a_1	χ^2/N
q	0.952	-70(305)	4.53 (*)	0.34(9)	3×10^{-3}
q	0.974	243(285)	4.53 (*)	0.34(8)	1×10^{-3}
q	1.007	508(332)	4.53 (*)	0.36(7)	2×10^{-2}
q	1.030	570(587)	4.53 (*)	0.37(15)	1.4×10^{-2}
q	1.065	544(790)	4.53 (*)	0.38(15)	6×10^{-2}
q	1.127	502(829)	4.53 (*)	0.39(15)	1×10^{-1}
q	1.261	23(1733)	4.53 (*)	0.46(25)	2×10^{-2}
f	0.73	29(61)	3.5 (*)	0.20(7)	$N = 0$
f	0.94	5(70)	3.5 (*)	0.33(7)	0.01
f	1.02	153(80)	3.5 (*)	0.37(7)	0.1
f	1.18	-10(40)	3.5 (*)	0.53(6)	1.9
f	1.48	-110(80)	3.5 (*)	0.55(6)	1.2

FIGURE CAPTIONS

Fig. 1. The quantity $\mathcal{D}_{\parallel}^E$ [Eq. (3.1)], in units of MeV^4 , versus the physical distance (in fm), for different values of T/T_c in the *quenched* theory. The thick continuum line has been obtained using the parameters of the best fit to the data at $T = 0$ [Ref. [8], Eqs. (2.10) and (2.11)].

Fig. 2. The quantity \mathcal{D}_{\perp}^E [Eq. (3.1)], in units of MeV^4 , versus the physical distance (in fm), for different values of T/T_c in the *quenched* theory. The thick continuum line has been obtained using the parameters of the best fit to the data at $T = 0$ [Ref. [8], Eqs. (2.10) and (2.11)].

Fig. 3. The quantity $\mathcal{D}_{\parallel}^B$ [Eq. (3.2)], in units of MeV^4 , versus the physical distance (in fm), for different values of T/T_c in the *quenched* theory. The thick continuum line has been obtained using the parameters of the best fit to the data at $T = 0$ [Ref. [8], Eqs. (2.10) and (2.11)].

Fig. 4. The quantity \mathcal{D}_{\perp}^B [Eq. (3.2)], in units of MeV^4 , versus the physical distance (in fm), for different values of T/T_c in the *quenched* theory. The thick continuum line has been obtained using the parameters of the best fit to the data at $T = 0$ [Ref. [8], Eqs. (2.10) and (2.11)].

Fig. 5. The quantity $\mathcal{D}_{\parallel}^E$ [Eq. (3.1)], in units of MeV^4 , versus the physical distance (in fm), for different values of T/T_c and for $T = 0$ in full QCD.

Fig. 6. The quantity \mathcal{D}_{\perp}^E [Eq. (3.1)], in units of MeV^4 , versus the physical distance (in fm), for different values of T/T_c and for $T = 0$ in full QCD.

Fig. 7. The quantity $\mathcal{D}_{\parallel}^B$ [Eq. (3.2)], in units of MeV^4 , versus the physical distance (in fm), for different values of T/T_c and for $T = 0$ in full QCD.

Fig. 8. The quantity \mathcal{D}_\perp^B [Eq. (3.2)], in units of MeV^4 , versus the physical distance (in fm), for different values of T/T_c and for $T = 0$ in full QCD.

Fig. 9. The magnetic gluon condensate $G_2^{(mag)}(T)$ [see Eqs. (4.6) and (4.7)], in units of $G_2^{(mag)}(T = 0)$, versus T/T_c . The black circles refer to the *quenched* case, while the white circles refer to the full-QCD case.

Fig. 10. The electric gluon condensate $G_2^{(ele)}(T)$ [see Eqs. (4.6) and (4.7)], in units of $G_2^{(ele)}(T = 0)$, versus T/T_c . The notation is the same as in Fig. 9.

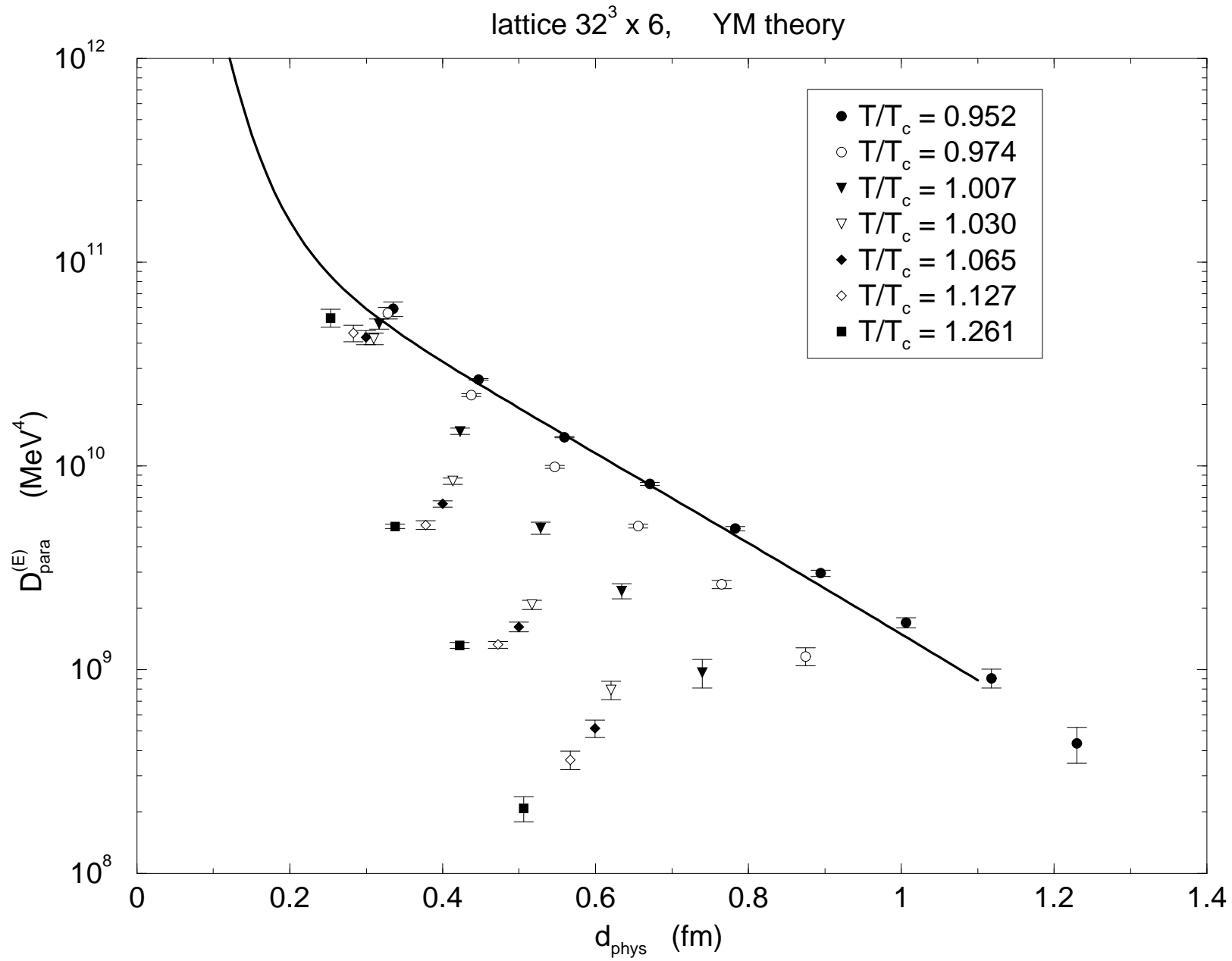


Figure 1

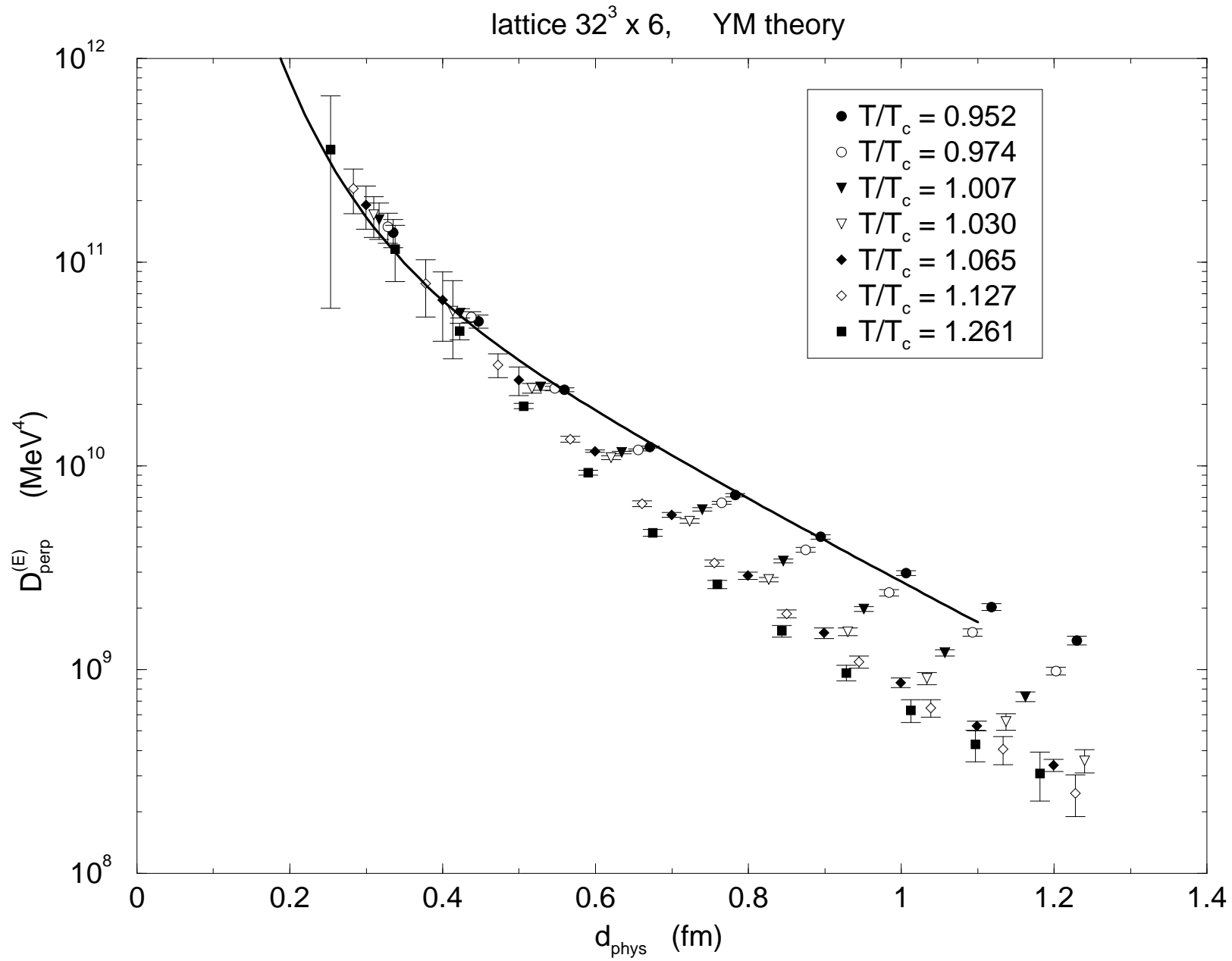


Figure 2

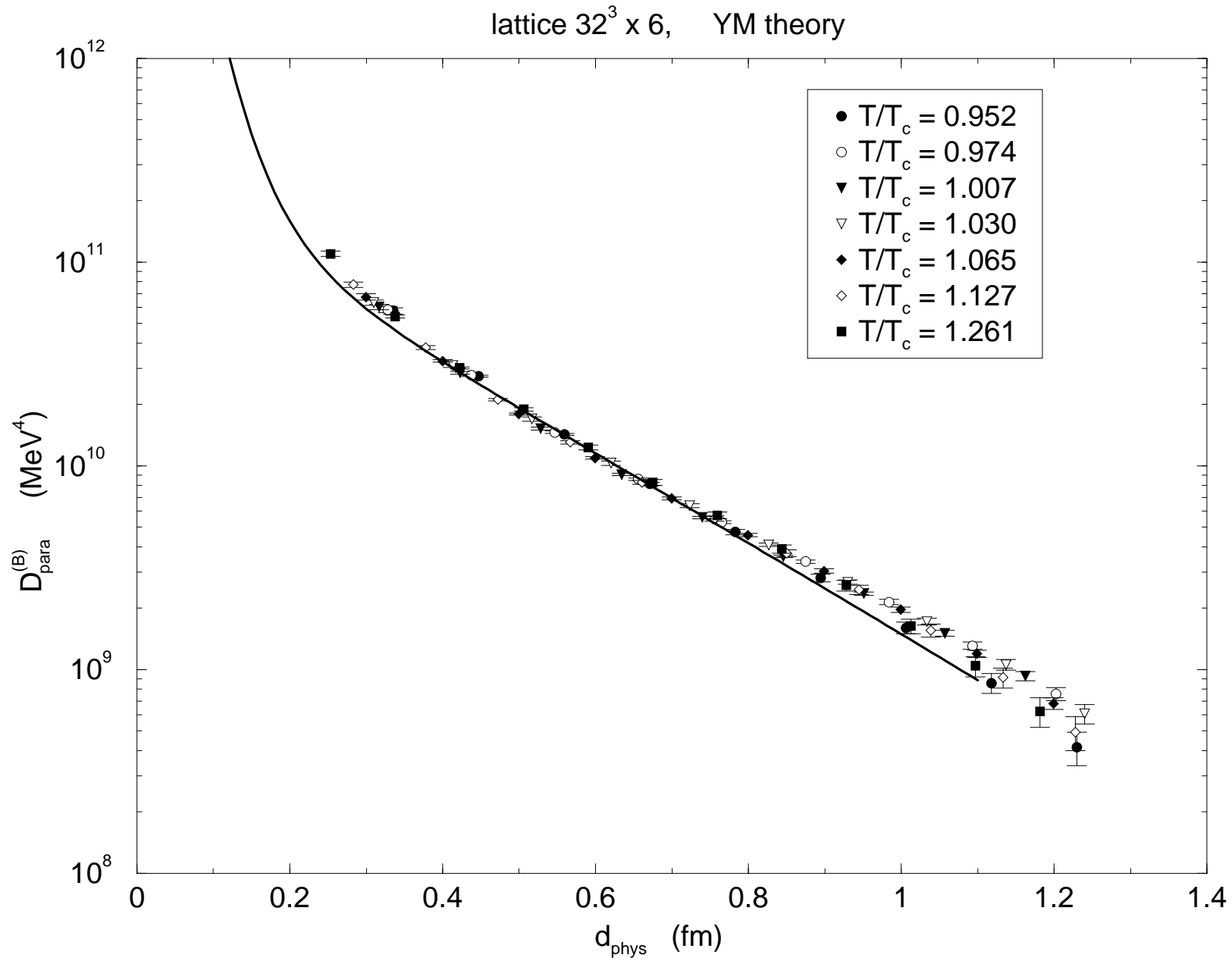


Figure 3

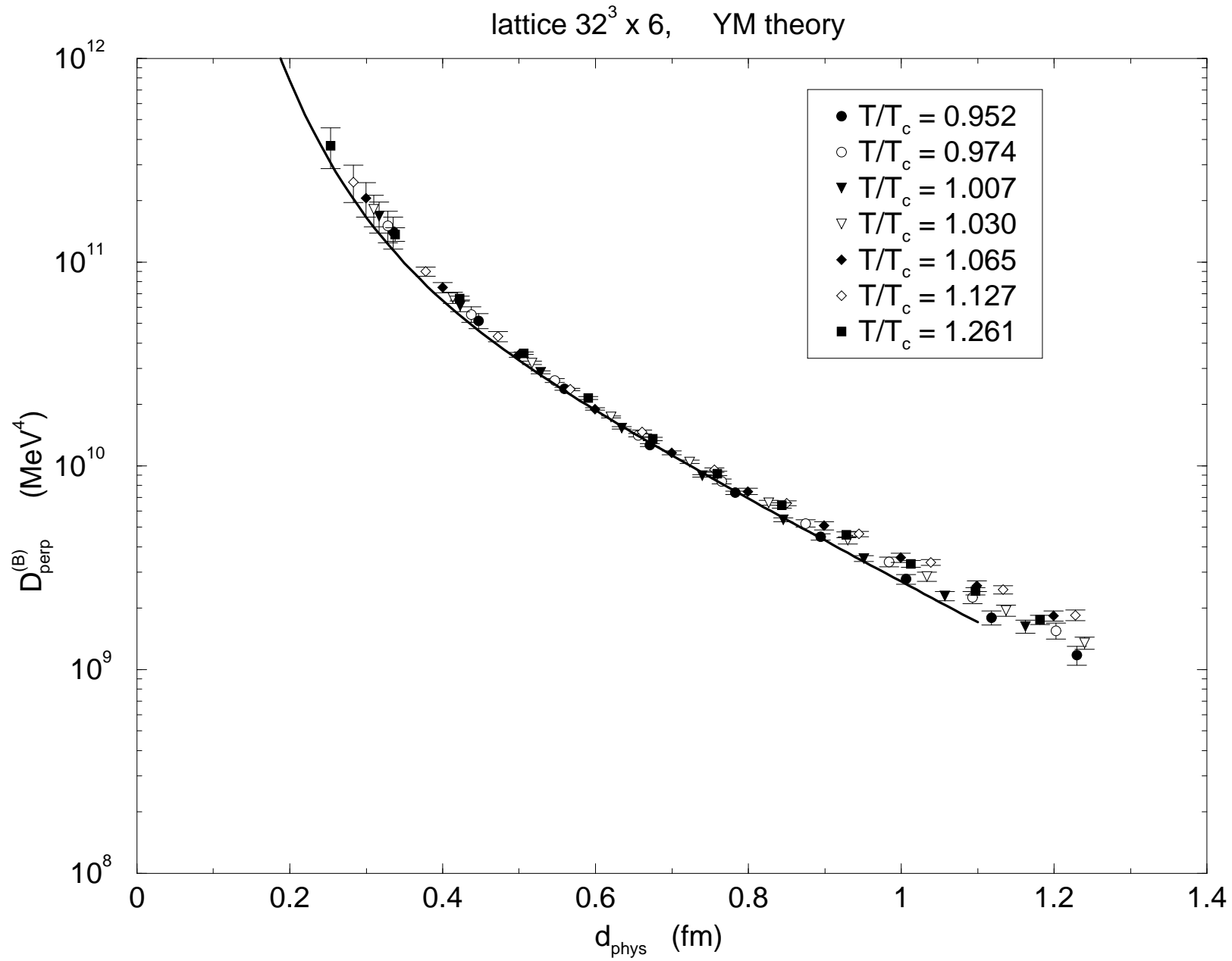


Figure 4

2 staggered flavours, $am = 0.0125$, lattice $32^3 \times 8$ and 16^4

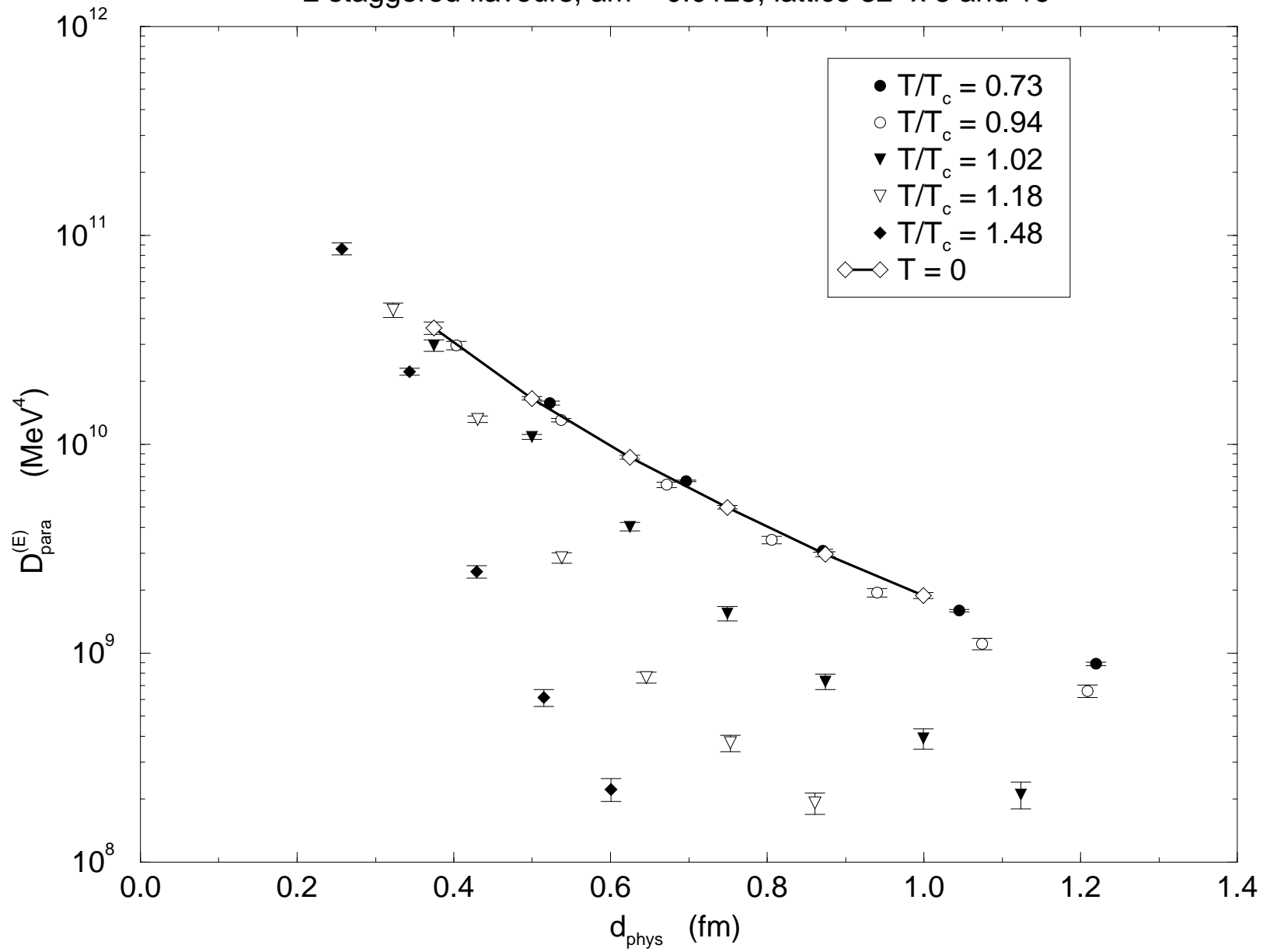


Figure 5

2 staggered flavours, $am = 0.0125$, lattice $32^3 \times 8$ and 16^4

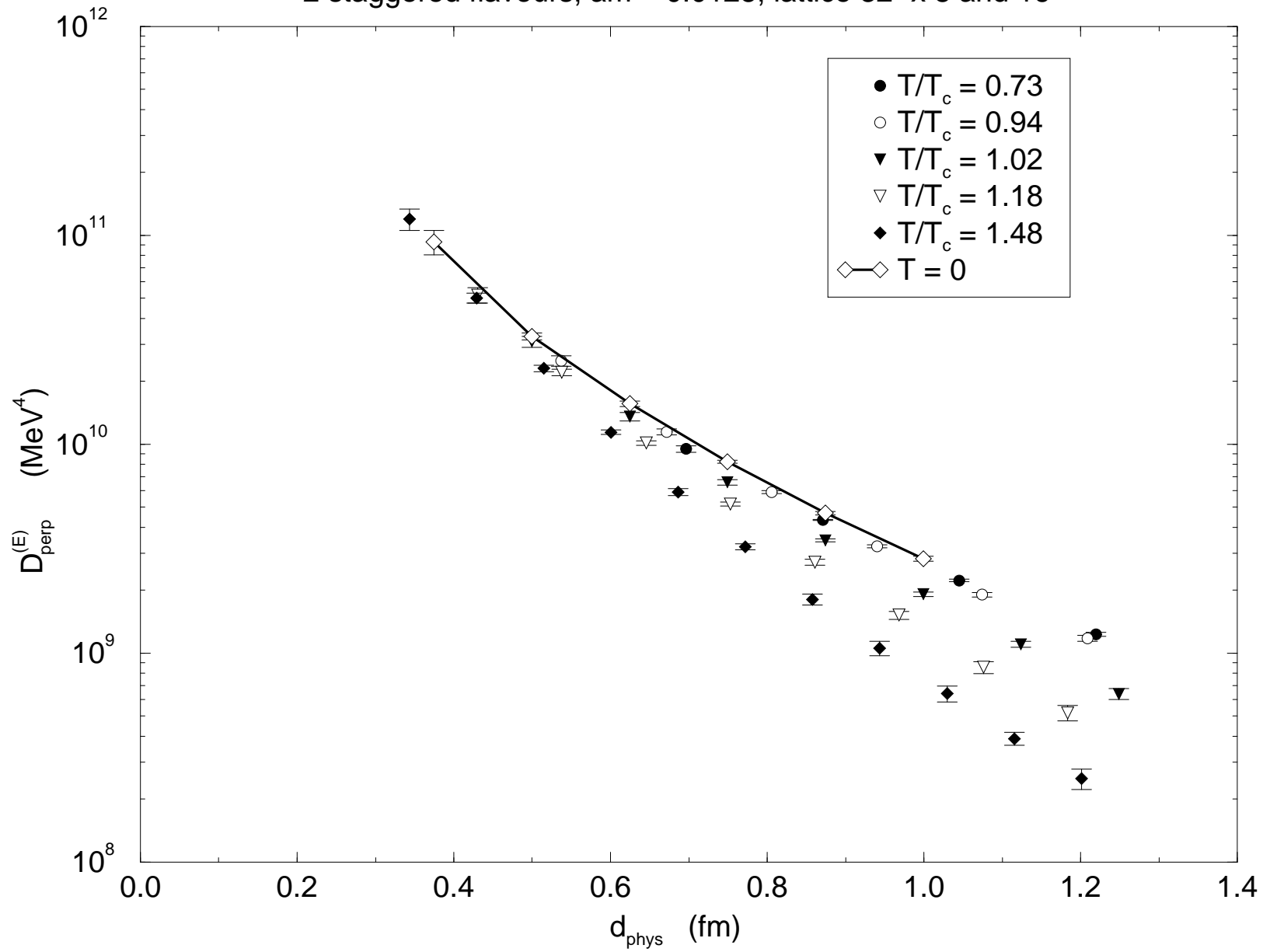


Figure 6

2 staggered flavours, $am = 0.0125$, lattice $32^3 \times 8$ and 16^4

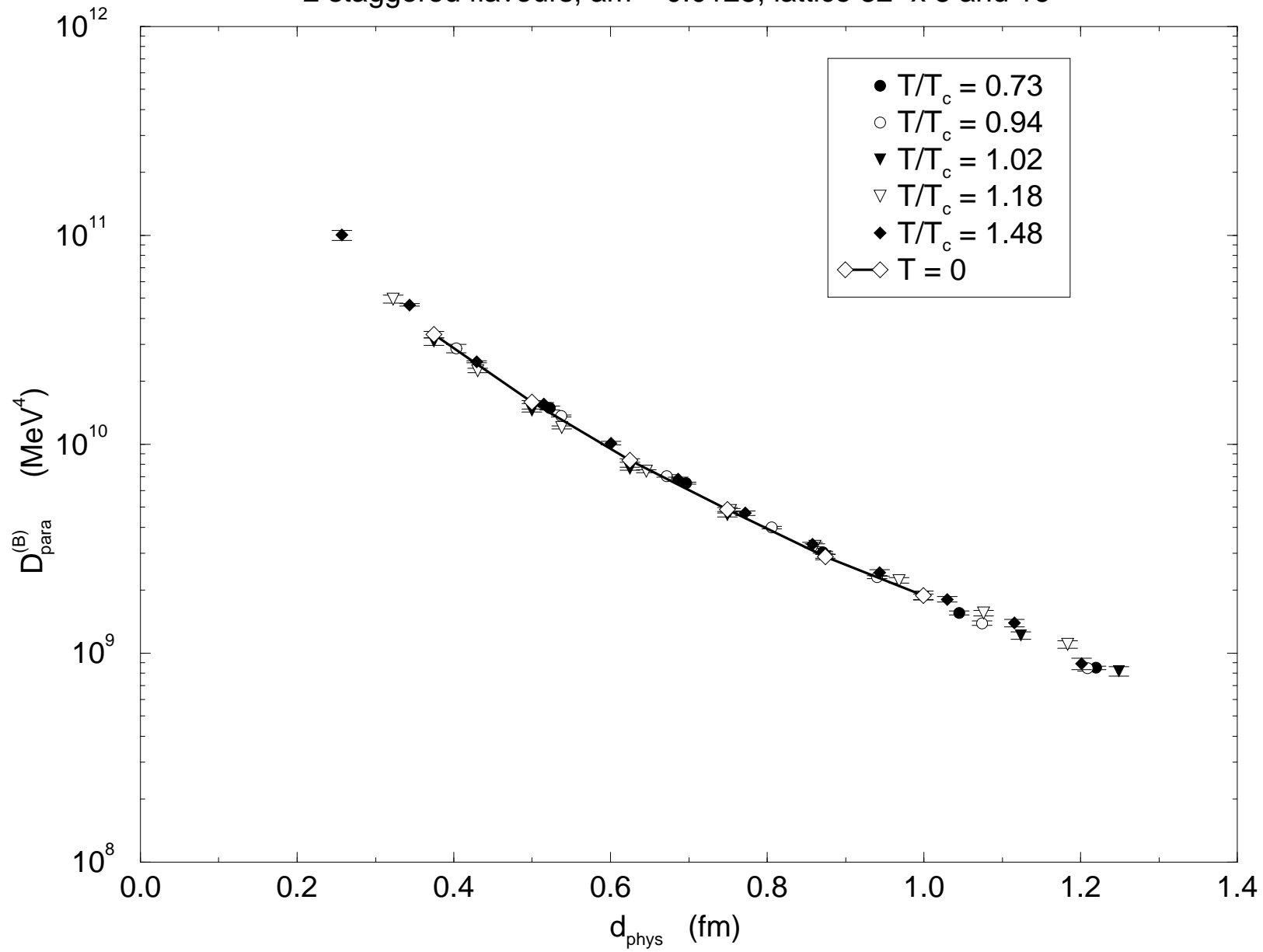


Figure 7

2 staggered flavours, $am = 0.0125$, lattice $32^3 \times 8$ and 16^4

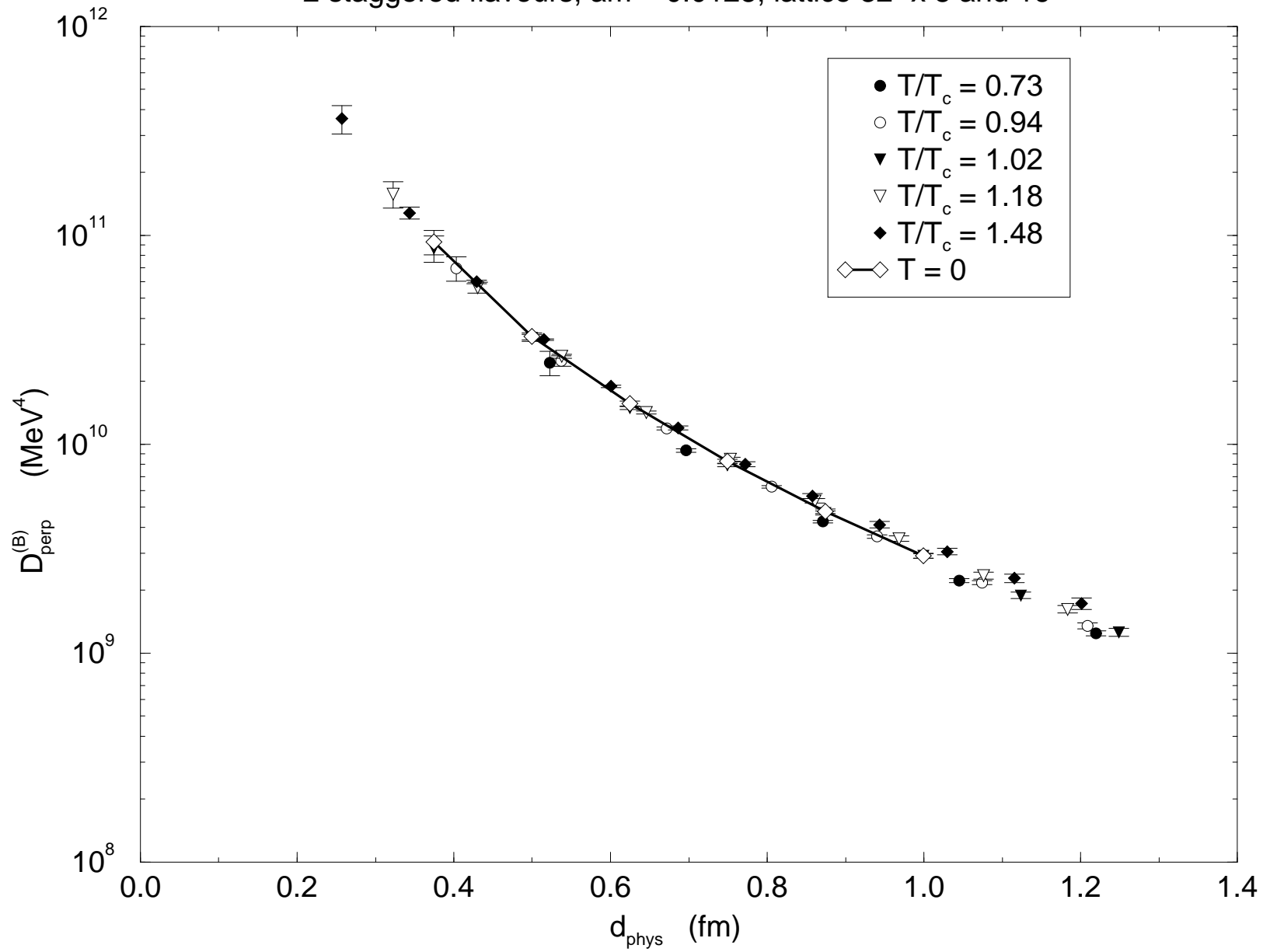


Figure 8

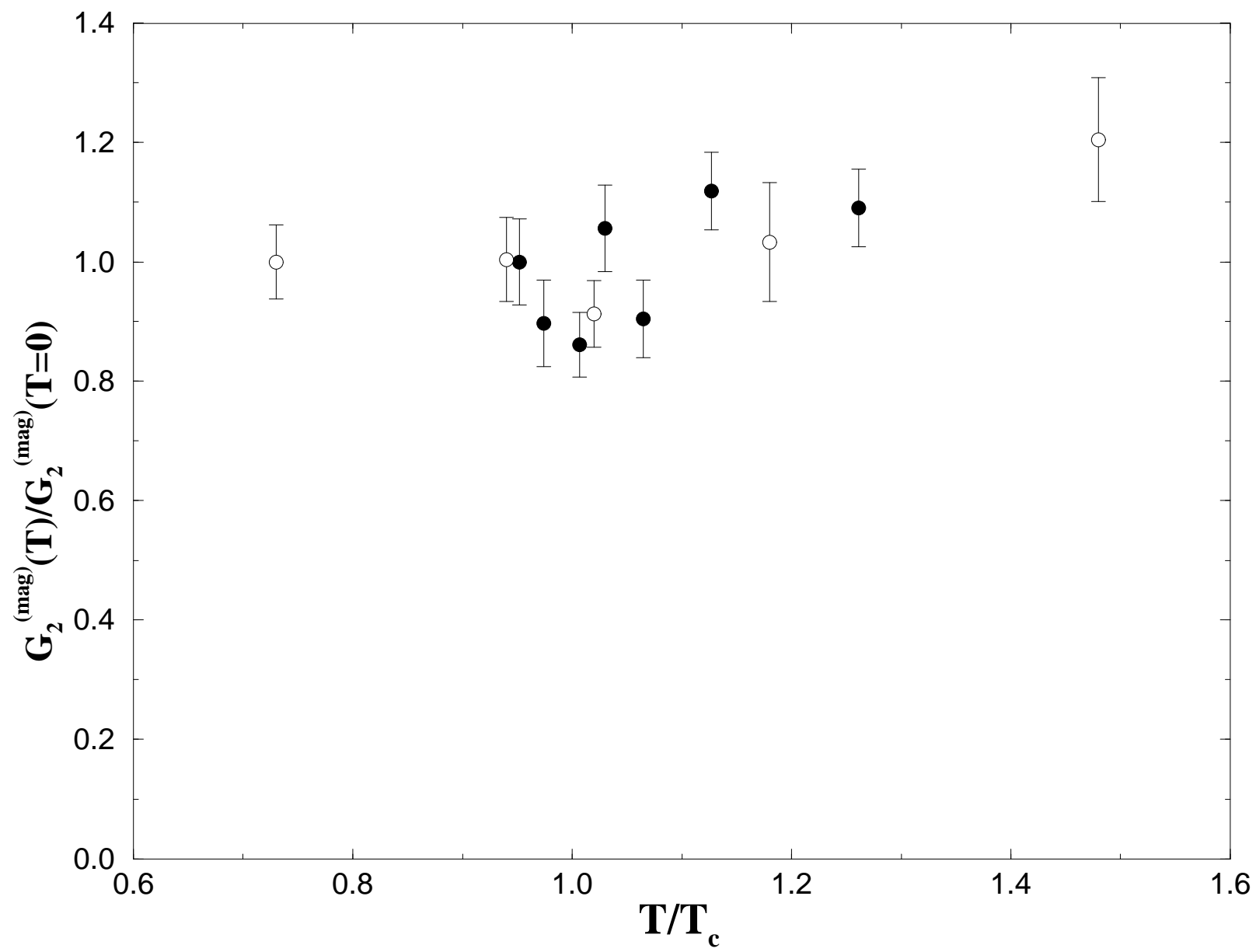


Figure 9

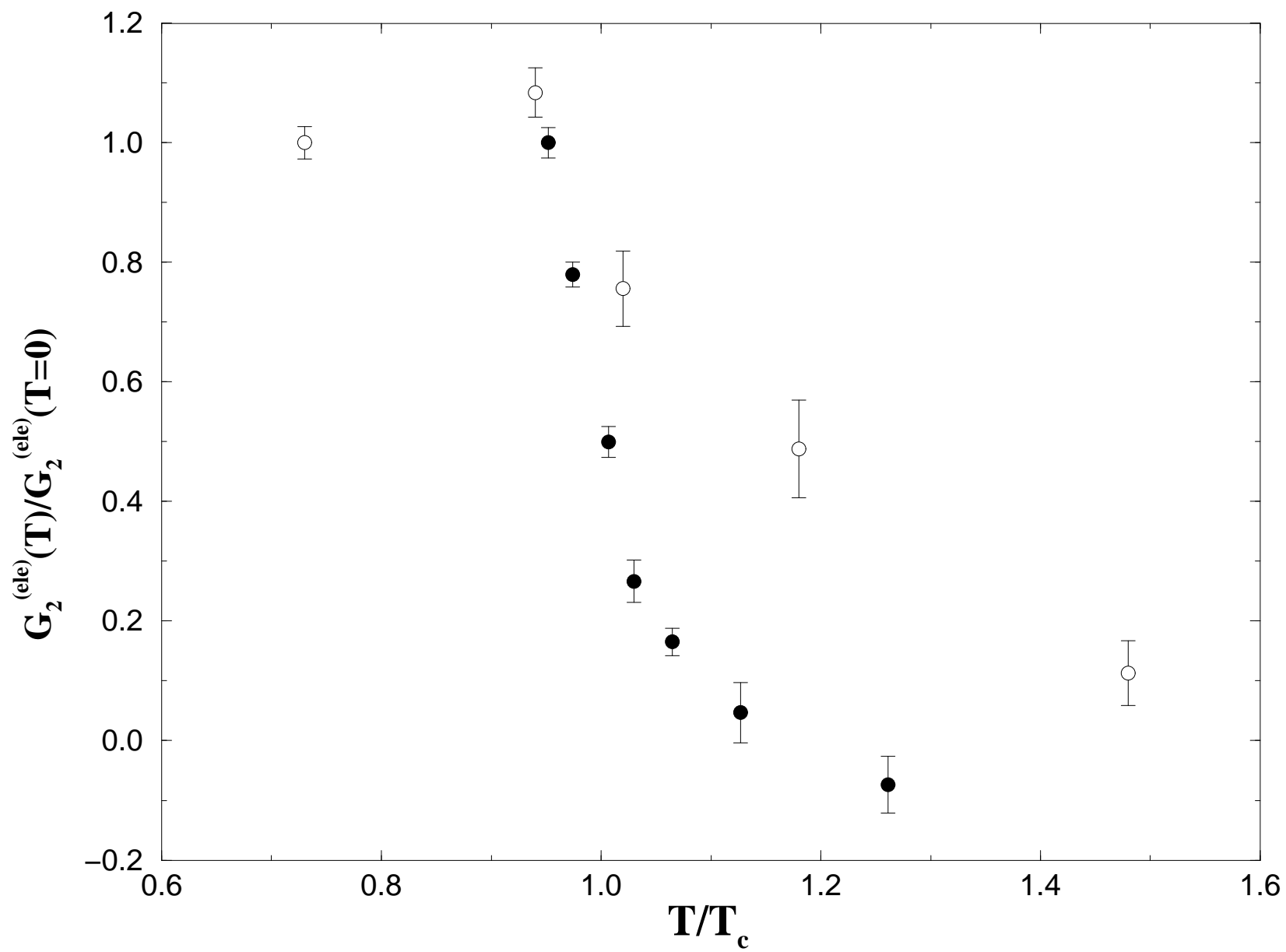


Figure 10